Achievable Information Rate for Outdoor Free Space Optical Communication with Intensity Modulation and Direct Detection

Jing Li (Tiffany)
Dept. of Electrical & Computer Engineering
Lehigh University
Bethlehem, PA 18015

Murat Uysal
Dept. of Electrical & Computer Engineering
University of Waterloo
Waterloo, Ontario N2L 3G1, Canada

Abstract— **This work investigates the achievable information rate with the state-of-the-art turbo coding and intensity modulation / direct detection for outdoor long-distance free-space optic (FSO) communications. The channel under weak atmospheric turbulence is modeled as a log-normal intensity fading channel where on-off keying makes it look asymmetric. While no effort is made to spectrally match the code to the asymmetry of the channel, the decoding strategy is optimally adjusted to match to the channel response. In addition to fixed rate turbo coding, a family of variable rate turbo codes are constructed and discussed. Shannon capacity is also briefly visited to denote the theoretic limit. It is shown that under low turbulence a single long turbo code is sufficient to get within 1 dB from the capacity, but when the turbulence gets strong, adaptive coding is necessary to close the gap. We expect these results to be useful for current and immediate future systems.**

I. Introduction

Free space optics (FSO), also known as wireless optics, is a cost-effective and high bandwidth access technique and receives growing attention with recent commercialization success. With the potential high data-rate capacity, low cost, convenient reconfigurability and scalability, high-security and particularly wide bandwidth on unregulated spectrum (as opposed to the limited bandwidth radio frequency (RF) counterpart), FSO systems have emerged as an attractive means for deep-space and intersatellite communication and other applications, e.g., search and rescue operations in remote areas.

This work considers outdoor long-distance FSO systems, in which optical transceivers communicate directly through air along point-to-point line-of-sight (LOS) FSO links. We first discuss the channel model under weak atmospheric turbulence, and then investigate the capacity of this channel. While capacity computation is useful in providing an ultimate limit of the system performance, it should be noted that performance evaluation is application specific. Hence, depending on the nature of the application, different types of capacities for fading channels have been defined in literature. For non-real-time data services, ergodic capacity was developed, which determines the maximum achievable information rate averaged over all fading states. On the other hand, delay-limited capacity (which specifies the achievable information rate subject to a given (decoding) delay independent of the fading correlation status) is useful for real-time data services, and outage capacity (which determines the ϵ-achievable rate) is useful for block fading (or quasi-static fading) channels. In this paper, we investigate the ergodic capacity of turbulence-induced FSO link that is characterized by log-normal fading.

What makes the problem interesting is that we consider on-off keying (OOK). OOK is rarely used in wireless RF systems, and little work has been reported in terms of capacity and coding performance. With OOK, the received signal demonstrates different statistics depending on whether "1" (On signal) or "0" (Off signal) is transmitted, which makes the channel (or the output from the channel) appear asymmetric. It is worth mentioning that intensity-modulation/direct-detection (IM/DD) with OOK is the only practical modulation/detection scheme that has been deployed in commercial systems. Higher order modulation with heterodyne reception, such as phase shift keying (PSK) and Quadrature Amplitude Modulation (QAM), although possible, are rarely used in practice due to technical difficulties and high cost. Hence, we expect our result to be useful for current and immediate future systems.

In reality, the turbulence-induced fading channel has channel gains correlated in time. Here we consider the capacity averaged over all time with the assumption that ideal interleaving is performed over an infinitely long sequence. Thus, the channel is simplified to a memoryless, stationary and ergodic channel with independent and identically distributed (i.i.d.) channel gain. We consider three cases: channel state information (CSI) is available at the transmitter only, at the receiver only, and at both.

To evaluate the channel characteristics, we also examine the outage rate of this outdoor FSO channel. We compare it to that of RF Rayleigh fading channels to illustrate its relative "goodness". To give a feel of how much can be achieved with the state-of-the-art forward error control (FEC) coding schemes, we evaluate turbo codes. In addition to fixed rate codes, a variable rate adaptive turbo coding scheme is also presented and discussed. We show that variable rate codes are more efficient in bandwidth and power, and that it is indispensable to employ adaptive coding and/or power control in order to get close to the capacity throughput under (relatively) strong turbulence.

The rest of the paper is organized as follows. Section II briefly discusses the channel model as well as the Shannon capacity of this channel. Sections III and IV discuss fixed rate turbo coding and variable rate adaptive coding, respectively. Section V concludes the paper.

II. System Model

A. Long-Distance FSO Systems Using IM/DD

In an outdoor long-distance FSO system, optical transceivers communicate directly through the air via point-to-point line-of-sight (LOS) FSO links. The transmitter usually utilizes semiconductor lasers with broad bandwidth and high launch power and the receiver employs a transimpedance design combined with bootstrapping, such as (optically pre-amplified) PIN or avalanche photodiodes (APD) of different dimensions. Intensity modulation and direct detection using OOK is widely deployed to modulate the signals.

The power budget and raw-data performance of a LOS FSO link are subject to atmospheric loss and interference along the propagation path, which includes free space loss, clear air absorption, scattering, refraction, atmospheric turbulence (also termed scintillation), and interference from ambient light (i.e., stray light in addition to the wanted optical beam that reaches

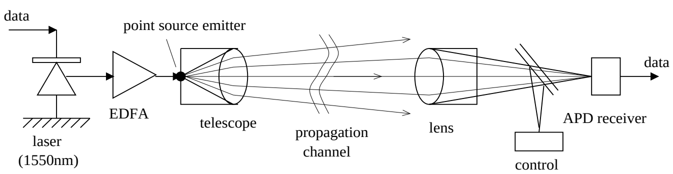

Fig. 1. A long-distance outdoor point-to-point FSO system. The propagation path schematically depicts free space loss.

photodiode). While ambient light can be quite strong (especially for indoor systems due to the large receiver aperture), by applying high-frequency sub-carriers, narrowband infrared filters, line codes and the like, its effect can be effectively removed [5] [7]. Free space loss, clear air absorption, scattering and refraction result in attenuation in the signal intensity, and field tests of major cities around the world show that the atmospheric attenuation of these factors is consistently low. For example, with a moderate power budget, 99.5% availability is achieved for 1km links at London, Manchester and Glasgow in UK [6]. Hence, these factors can be collectively modeled as a constant parameter (compared to turbulence) in the mathmatic model. The dominant impairment to long-distance outdoor systems (500m to a few kilometers) is atmospheric turbulence, which occurs as a result of the variation in the refractive index due to inhomogeneities in temperature and pressure fluctuations, and which causes random amplitude fluctuations in optical signals.

We follow the same mathematic description of the channel model as in [7] and [3]. Specifically, atmospheric turbulence is physically described by Kolmogorov theory [1] [2] and, at long distance and weak turbulence, takes log-normal statistics [3], [**?**]. The statistical channel model can be characterized as follows:

$$y = sx + n = \eta I x + n \qquad (1)$$

where $s = \eta I$ denotes the instantaneous intensity gain, $x \in \{0, 1\}$ the OOK modulated signal, $n \sim \mathcal{N}(0, N_0/2)$ the white Gaussian noise caused essentially by superposition of circuit noise and thermal noise in electronics, η the effective photocurrent conversion ratio of the receiver and I the turbulence-induced light intensity (normalized), which satisfies

$$I = \exp(2Z), \qquad (2)$$

where $Z \sim \mathcal{N}(0, \sigma_z^2)$. Hence, I takes a log-normal distribution with mean $e^{2\sigma_z^2}$, variance $e^{4\sigma_z^2}(e^{4\sigma_z^2}-1)$, and probability density function (pdf)

$$f_I(z) = \frac{1}{2z\sigma_z\sqrt{2\pi}}\, e^{-\frac{(\ln z)^2}{8\sigma_z^2}}. \qquad (3)$$

Conforming to [7], we define the average signal-to-noise ratio (SNR) using OOK as

$$\bar{\gamma}_0 = \frac{\eta^2 \mathrm{E}[I^2]\ \mathrm{E}[X^2]}{N_0} = \frac{\eta^2 e^{8\sigma_z^2}}{2N_0}. \qquad (4)$$

If binary phase shift keying (BPSK) instead of OOK were adopted, i.e., $x \in \{\pm 1\}$, the average SNR would be $\bar{\gamma}_1 = 2\bar{\gamma}_0$.

B. Shannon Capacity of Log-Normal FSO Channel

The Shannon capacity is defined as the maximum mutual information between the input to the channel, X, and output from the channel Y, where the maximum is taken over all input distribution. We consider binary input and continuous output:

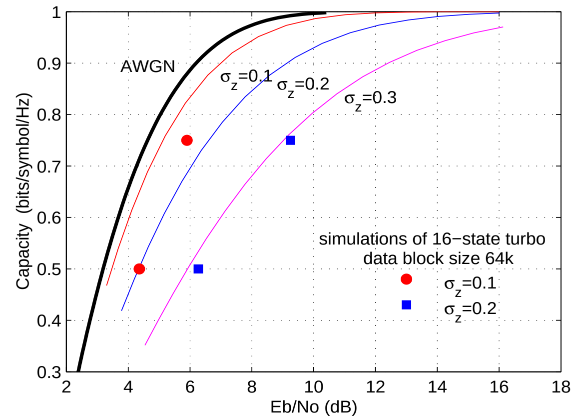

Fig. 2. Capacity of the log-normal fading FSO channel using OOK

$$C \triangleq \max_p(x) I(X;Y)) = \int_{-\infty}^{\infty} \sum_{x=0}^{1} \Bigg[p(x) f(y|x) \log \frac{f(y|x)}{\sum_{m=0}^{1} p(m) f(y|m)} \Bigg] dy \qquad (5)$$

Due to OOK signaling, signal experiences different amount of impairment depending on whether 0 or 1 is sent. Nevertheless, it has been shown in [7] that the optimal distribution is $p(x\!=\!0) = p(x\!=\!1) = 1/2$ as if the channel is symmetric. With perfect channel state information (CSI), the Shannon capacity of this FSO channel is given by [7]

$$C(\bar{\gamma}_0) = \int_{-\infty}^{\infty} C_{\mathrm{AWGN}}(s, N_0) f_s(s)\, ds, \qquad (6)$$

where $\bar{\gamma}_0$ is the average SNR given in (4), $f_s(s) = f_I(s/\eta)$ in (3), and $C_{\mathrm{AWGN}}(s, N_0)$ is the capacity of the equivalent AWGN channel with binary input $\{0, s\}$ and Gaussian noise variance $N_0/2$, which, in turn, is equivalent to the capacity of the well-known BPSK AWGN channel evaluated at SNR of $\frac{s^2}{4N_0}$.

Fig. 2 plots the capacity curves along with that of a non-fading AWGN channel (OOK assumed for all cases), where the x-axis denotes the normalized bit SNR $E_b/N_0 = \bar{\gamma}_0/C$. Apparently, the AWGN case is the limit of the log-normal fading case as $\sigma_z \to 0$. It is observed that the channel capacity decreases considerably as atmospheric turbulence gets strong ($\sigma_z = 0.1$ to 0.3). It is also interesting to note that atmospheric turbulence incurs a bigger loss in E_b/N_0 at high rates than at low rates. This suggests that atmospheric turbulence can be a more detrimental factor for achieving high channel throughput than low throughput (assuming capacity-approaching coding is equally difficult for low and high rates alike).

III. Fixed Rate Turbo Coding With Side Information

While optical domain techniques are widely exploited, electrical domain techniques are just starting to apply to the optical systems. To shed light upon how much can be achieved with the state-of-the-art error control coding schemes, we evaluate the performance of the best known codes. Two turbo code are considered, whose generator polynomials of the component recursive systematic convolutional (RSC) codes are given by $[1, (1+$

$D^2+D^3+D^4)/(1+D+D^4)]$ and $[1, (1+D^2)/(1+D+D^2)]$, respectively. The former is one of the best 16-state turbo codes and has been shown to perform remarkably on a variety of channels including the RF Rayleigh fading channels and the long-haul fiber-optic channels. The latter is a 4-state turbo code that is (relatively) simple yet still well-performing. We assume independent fading with perfect CSI known to the receiver. The original turbo code with 2 parallel branches have code rate 1/3, and alternating uniform puncturing on parity bits are used to obtain higher rates.

The decoder of the turbo codes uses the well-known iterative decoding strategy with soft-in soft-out sub-decoders for component codes. We employ the maximum *a posteriori* probability (APP) decoder (the BCJR algorithm) as sub-decoders. For optimal performance, the BCJR algorithm needs to be modified to incorporate the underlying channel characteristics. Denote

$$\mathbf{a} \triangleq a_1^N = (a_1, a_2, \cdots, a_t, \cdots, a_N), \quad (7)$$

$$\mathbf{X} \triangleq X_1^N = (X_1, X_2, \cdots, X_t, \cdots, X_N), \quad (8)$$

$$\mathbf{Y} \triangleq Y_1^N = (Y_1, Y_2, \cdots, Y_t, \cdots, Y_N), \quad (9)$$

as the input sequence to the RSC encoder (user data), output sequence at the RSC encoder (coded/modulated bits), and the output sequence from the channel (noise corrupted bits), respectively. It should be noted that for a rate $1/k$ convolutional (component) code, both Y_t and X_t are vectors of k symbols.

Recall that the the BCJR algorithm involves the computation of three parts: the transition branch metric γ_t, the forward path metric α_t and the backward path metric β_t [10]. α_t and β_t are computed through forward and backward recursions, which remain the same irrespective of channel model:

$$\begin{aligned} \alpha_t(m) &\triangleq P(\,S_t\!=\!m,\, Y_1^t\,), \\ &= \sum_{m',a_t} \alpha_{t-1}(m')\,\gamma_t(a_t, m', m), \end{aligned} \quad (10)$$

$$\begin{aligned} \beta_t(m) &\triangleq P(\,Y_{t+1}^N \,|\, S_t\!=\!m\,), \\ &= \sum_{m',a_t} \beta_{t+1}(m')\,\gamma_{t+1}(a_t, m, m'), \end{aligned} \quad (11)$$

where S_t denotes the trellis state at time instant t.

The computation of γ_t, however, needs to account for the underlying channel. Specifically, the transition metric associated with the branch from state m' to m at time instant t is given by

$$\begin{aligned} &\gamma_t(a_t, m', m) \triangleq P(\,a_t, S_t\!=\!m, Y_t \,|\, S_{t-1}\!=\!m'\,) \\ &= P(\,a_t \,|\, S_t\!=\!m,\, S_{t-1}\!=\!m'\,)\cdot P_{ap}(a_t)\cdot P(\,Y_t \,|\, X_t\,). \end{aligned} \quad (12)$$

The first term in (12) is either 1 or 0 depending on whether or not a_t is the information bit that is associated with the transition from m' to m, and is solely dependent on the trellis structure. The second term is the *a priori* probability of user bit a_t, and in the context of turbo codes, is the extrinsic information passed along from the other sub-decoder about bit a_t. The third term is closely related to the underlying channel as well as the modulation scheme in use. For OOK on log-normal fading FSO channel, it is given by

$$P(\,Y_t \,|\, X_t\,) = D\cdot \exp\left(\frac{2\eta I_t}{N_0} < Y_t, X_t > \right) \quad (13)$$

where $< Y_t, X_t >$ stands for the inner product of Y_t and X_t, D is a constant that has no real impact on the soft output, and X_t is a sequence of $\{0, 1\}$ bits (rather than ± 1 as in the conventional BPSK case).

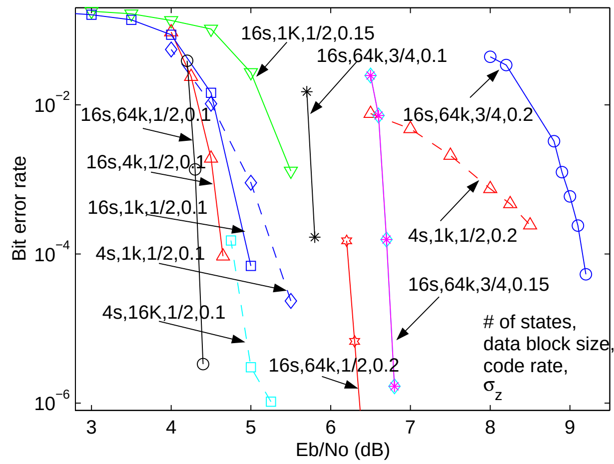

Fig. 3. Turbo codes with different parameters on FSO channels

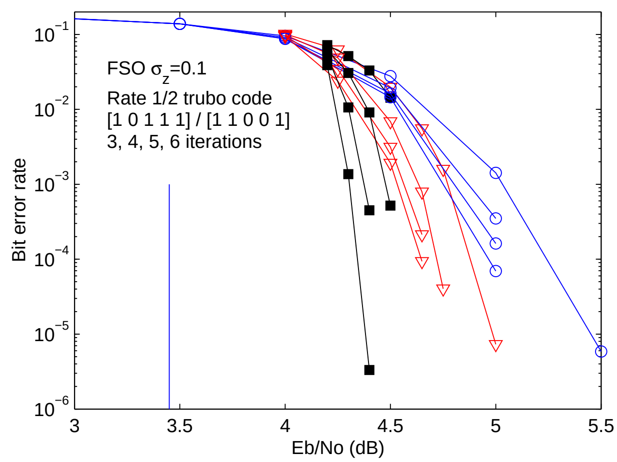

Fig. 4. 16-state rate 1/2 turbo codes on FSO channels

When the computation of γ_t is well matched to the channel, the overall log likelihood ratio (LLR) of a bit can then be computed using

$$\begin{aligned} L(a_t) &\triangleq \log \frac{\Pr(\,a_t\!=\!0 \,|\, Y_1^N\,)}{\Pr(\,a_t\!=\!1 \,|\, Y_1^N\,)}, \\ &= \log \frac{\sum_{m,m'} \alpha_{t-1}(m)\,\gamma_t(a_t\!=\!0, m, m')\,\beta_t(m')}{\sum_{m,m'} \alpha_{t-1}(m)\,\gamma_t(a_t\!=\!1, m, m')\,\beta_t(m')}. \end{aligned} \quad (14)$$

Apparently, the probability of bit a_t being 0 or 1 (at the decoder of a sub- RSC code) is given by $P(\,a_t=0 \,|\, Y_1^N\,) = \frac{e^{L(a_t)}}{1+e^{L(a_t)}}$, and $P(\,a_t\!=\!1 \,|\, Y_1^N\,) = \frac{1}{1+e^{L(a_t)}}$.

The performance of turbo codes with decoder matched to FSO channels is plotted in Fig. 3 and 4. Extensive simulation is conducted to benchmark the performance of turbo codes with different rates, lengths, complexities and under different turbulence strengths (Fig. 3). Each curve is marked with 4 parameters indicating the number of states (of the component code), the data block size, the code rate, and σ_z of the atmospheric turbulence, respectively.

Fig. 4 evaluates the 16-state rate 1/2 turbo codes. Block sizes from small to large are evaluated which reveals the interleaving gain phenomenon (K=1k, 4K, 64K). Bit error rate after 3, 4, 5, 6 iterations are shown to demonstrate how the number of decoding iterations (i.e. complexity and delay) affect the performance.

To see how close we are from the capacity limit, we also plot in Fig. 2 the simulation results of long turbo codes (64K), The performance is evaluated at BER of 10^{-5} with 6 decoding iterations. Under weak atmospheric turbulence ($\sigma_z = 0.1$), we see that 16-state turbo codes with fairly large block sizes can perform within 1 dB from the capacity. However, as turbulence strength increases, the same code performs farther away from the capacity. This should not be a surprising result, since under severe amplitude fluctuation, a larger block size (i.e. a stronger code and a longer time averaging) is generally needed to achieve the same level of performance. The plot also implies that under strong turbulence, using powerful FEC codes alone is not sufficient to achieve near-capacity performance, and that adaptive coding and/or optimal power control seem necessary in order to close the gap.

Although not shown, we have also tested the performance of low density parity check (LDPC) codes, which are known to perform as well as, and in some cases better than, turbo codes. Both regular LDPC (column weight 3) and irregular LDPC that are optimized for AWGN channels are tested. The performance of LDPC codes are (noticeably) worse than turbo codes. The implication of this experiment is two-fold: (i) turbo codes are quite stable and robust, and thus are a safe choice for a variety of channels; (ii) LDPC codes, although capable of performance within 0.0045 dB from the capacity limit on AWGN channel [**?**], are sensitive to channel characteristics and require specific design and optimization (matched to the channel) in order to achieve near-capacity performance. Code design is a hot research topic. It will be particularly interesting yet challenging to design LDPC codes for FSO channels due to the asymmetric channel characteristics caused by OOK signaling.

IV. Variable Rate Adaptive Coding

Since fixed rate coding fails to exploit the time-varying nature of the FSO channels and, hence, is not efficient in achieving the maximum information rate under large amplitude fluctuations. To achieve higher data rates and higher spectrum efficiency, we investigate variable rate adaptive coding for outdoor FSO communications. To ease the analysis, we assume that an error-free, zero-delay feed-back channel is available. Further, we conform to the specifications of the rate adaptation for packet data services in 2nd and 3rd generation cellular standards like GPRS, CDMA IS-95 Rev B and CDMA2000, and assume that the measurement report in the feedback message includes bit error rate and signal variance (or pilot strength measurement). Hence the transmitter can adapt to the changing channel conditions, sending more information with less error protection to achieve higher throughput when channel conditions are good, but using more powerful codes to ensure transmission reliability when channel conditions become worse.

For efficient rate adaptive coding, the following properties are desired:

- *Rate compatibility* so that only a single encoder and decoder pair is required to deploy a class of variable rate FEC codes;
- *Constant bandwidth* to ensure smooth transmission and stable buffer utilization as the payload throughput changes.
- *Large minimum distance* for good performance even with high rate codes.

We use turbo codes in the design of variable rate adaptive coding scheme. The nice thing about turbo codes is that high-rate (yet still well-performing) codes can be obtained by puncturing from low-rate mother code. This makes it convenient to archive rate compatibility where the same encoder/decoder pair can be used. Note this is not readily obtainable with LDPC codes, where the change of code rate and/or length typically requires a reconstruction of the parity check matrix[1]. Since puncturing generally decreases the minimum distance of a code, we use 16-state turbo codes as the mother code, whose relatively long constraint length (yet still practical complexity) would alleviate the negative impact of puncturing. The same generator polynomial as in the previous section will be used, $[1, (1+D^2+D^3+D^4)/(1+D+D^4)]$. The recursive feedback polynomial therein is primitive, and we expect this code to result in good free distance as well as good effective free distance [8], the latter of which is particularly important for punctured (turbo) codes to still exhibit good performance and low error floors.

To achieve constant bandwidth usage, the variable rate coding scheme requires the input data block size to be changeable. Recall that in a rate (N, K) turbo code, an interleaver of size K is used to scramble the data bits before they are fed into the second component code. Hence, for a set of rates $R = K_1/N$, K_2/N, $\cdots$, K_m/N, m interleavers of size K_1, K_2, $\cdots$, K_m need to be stored, which may cause serious problem in memory/space. Among the possible candidate interleavers, block interleavers are known for their simplicity and on-the-fly interleaving, but the "rectangular error pattern" in a block interlever could cause high error floors especially for short block sizes and punctured codes. For steeper curve and lower error floors, random interleavers and particularly S-random interleavers are desired. However, interleaving and deinterleaving therein use look-up tables, which can be quite inefficient in hardware. Further, the need to store several interleavers makes them very expensive (and practically infeasible) for use in a multiple rate coding system. For this reason, we explore algebraic interleavers in our design for variable rate codes. With an algebraic interleaver, the interleaving pattern can be generated pseudo-randomly on the fly without having to store the interleaving pattern. We consider congruential sequence which can be generated using the following rule [9]

$$A_{n+1} = (a \cdot A_n + b) \bmod N. \tag{15}$$

To ensure that (15) generates a maximal length sequence from 0 to $N-1$, parameters a and b need to satisfy

- $a < N,\ b < N,\ b$ be relatively prime to N;
- (a-1) be a multiple of p, for every prime p dividing N;
- (a-1) be a multiple of 4 if N is a multiple of 4.

It is also desirable, although not essential, to have

- a be relatively prime to N.

This method is similar to what is used to in a computer to generate "pseudo-random" numbers. Empirical results show that for most values of a, b and A_0 that satisfy the above conditions,

[1]Although puncturing is also possible with LDPC codes, the number of bits that can be punctured is very limited or the performance will deteriorates drastically. [12] proposed a way of combining both puncturing and extending to construct efficient rate compatible LDPC codes whose parity check matrices take a special form.

the resulting interleaver exhibits good "randomness" akin to a random interleaver. Since only the values of a, b and A_0 need to be stored, algebraic interleaving is cheap to implement and flexible to change code rate and/or length and, hence, desirable for variable-rate or multi-rate codes.

We conduct computer simulations to evaluate the performance of the proposed variable rate turbo coding scheme. We fix codeword length to be $N = 8$K, and allow the encoder to adaptively select, according to the channel measurement information received in the feedback channel, one of the following rates: $R = 1/3$, 1/2, 2/3, 3/5 and 3/4. Fig. 5 plots the BER performance curves of the class of variable rate turbo codes constructed using puncturing and algebraic interleaving. We see that each code is itself a powerful FEC code, and they collectively can achieve incremental performance improvement, thus permitting low error probability over a large dynamic range of (instantaneous) SNRs.

To see how adaptive coding performs, we use the following rate adaption rule:

$$\text{Selecting rate } R = \begin{cases} 1/3, & \gamma_0 \leq 6.5 \text{ dB} \\ 1/2, & 6.5 < \gamma_0 \leq 7.5 \text{ dB} \\ 3/5, & 7.5 < \gamma_0 \leq 8.4 \text{ dB} \\ 2/3, & 8.4 < \gamma_0 \leq 9.5 \text{ dB} \\ 3/4, & \gamma_0 > 9.5 \text{ dB} \end{cases}$$

where γ_0 denotes the instantaneous SNR (E_b/N_0) using OOK. It should be noted that, due to the lack of formal methods, the above adaption rule is not optimized, but is chosen by way of observation. Nevertheless, simulations show an admissible performance with this adaption rule.

Fig. 6 plots the throughput of the rate adaptive turbo codes on FSO channels, where the throughput is computed by averaging the data information rate (at BER of 10^{-5}) over a very long observation time. We choose $\sigma_z = 0.2$, which, as shown before, results in relatively strong atmospheric turbulence that caused a single fixed-rate long turbo code to perform beyond 2 dB from the capacity (Fig. 2). As we can see from Fig. 6, the much shorter variable rate turbo code can close the gap by an additional 0.8 dB, which is quite encouraging. The rate adaptive coding scheme in use has a flavor of frame-by-frame power adaptation. In order to get further close to the capacity limit, we expect that (optimal) symbol-by-symbol power allocation is needed.

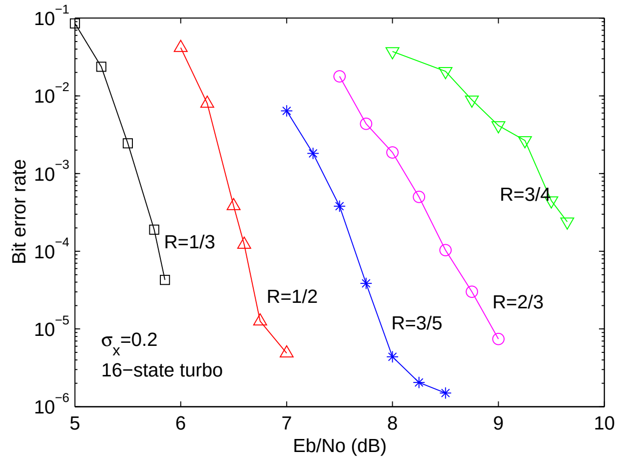

Fig. 5. A set of variable rate turbo codes with codeword length 8K.

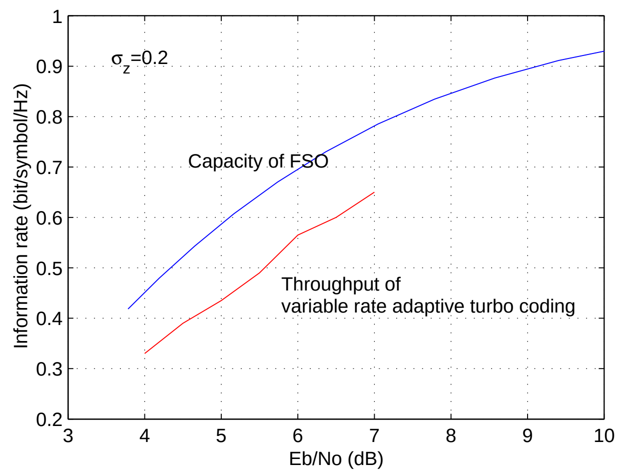

Fig. 6. Throughput of variable rate adaptive coding.

V. Conclusion

We consider an outdoor long-distance FSO channel with IM/DD using OOK. The channel is modeled as an ergodic memoryless log-normal fading channel. State-of-the-art turbo codes are investigated to demonstrate how much has been achieved. The conventional BCJR algorithm is modified to match to the channel characteristics. Both fixed rate turbo coding and variable rate adaptive coding are evaluated. We show that under weak turbulence, a single long turbo codes are capable of performance within 1 dB from the capacity limit. However, as turbulence gets stronger, adaptive coding and (optimal) power allocation is necessary in order to get close to the capacity.

References

[1] A. Ishimaru, *Wave Propagation and Scattering in Random Media*, Academic, NY, 1978, vol. 1-2.

[2] S. Karp, R. Gagliardi, S. E. Moran, and L. B. Stotts, *Optical Channels*, Plenum, NY, 1988.

[3] X. Zhu and J. M. Kahn, "Free-space optical communication through atmospheric turbulence channels," *IEEE Trans. Commun.*, vol. 50, pp. 1293-1300, Aug. 2002.

[4] X. Zhu and J. M. Kahn, "Performance Bounds for Coded Free-Space Optical Communications through Atmospheric Turbulence Channels," to appear in *IEEE Trans. on Commun.*

[5] D. J. T. Heatley, D. R. Wisely, I. Neild, and P. Cochrane, "Optical wireless: the story so far," *IEEE Commun. Mag.*, pp. 72-74, 79-82, Dec. 1998.

[6] P. Smyth *et al.*, "Optical wireless–a prognosis," *Proc. SPIE*, 1995.

[7] J. Li, and M. Uysal, "Optical wireless communications: system model, capacity and coding," *Proc. Vehicular Tech. Conf.*, to appear, Orlando, Florida, Oct. 2003.

[8] S. Benedetto and G. Montorsi, "Unveiling turbo codes: some results on parallel concatenate coding schemes," *IEEE Trans. Inform. Theory*, IT-42, pp. 409-428, Mar., 1996.

[9] G. C. Clark, Jr. and J. B. Cain, *Error-correction coding for digital communications*, Plenum Press, NY, 1981.

[10] L. R. Bahl, J. Cocke, F. Jelinek, and J. Raviv, "Optimal decoding of linear codes for minimizing symbol error rate," *IEEE Trans. Inform. Theory*, vol. 20, pp. 284-287, Mar. 1974.

[11] S.-Y. Chung, G. D. Forney, T. J. Richardson and R. Urbanke, "On the design of low-density parity-check codes within 0.0045 dB of the Shannon limit," *IEEE Commun. Let.*, vol. 5, pp. 58-60, Feb. 2001.

[12] J. Li, K. R. Narayanan, and C. N. Georghiades, "Rate-compatible low density parity check codes for capacity-approaching ARQ schemes in packet data communications," *Proc. Intl. Conf. on Commun., Internet and Inform. Tech.*, US Virgin Islands, pp. 201-206, Nov. 2002.